Dynein Light Chain LC8 Negatively Regulates NF-κB through the Redox-dependent Interaction with IκBα*

Yuyeon Jung[1], Hojin Kim[1], Sun Hee Min, Sue Goo Rhee[2], and Woojin Jeong[3]

From the Department of Life Science, Division of Life and Pharmaceutical Sciences, and Center for Cell Signaling and Drug Discovery Research, Ewha Womans University, Seoul 120-750, Korea

Redox regulation of nuclear factor κB (NF-κB) has been described, but the molecular mechanism underlying such regulation has remained unclear. We recently showed that a novel disulfide reductase, TRP14, inhibits tumor necrosis factor α (TNFα)-induced NF-κB activation, and we identified the dynein light chain LC8, which interacts with the NF-κB inhibitor IκBα, as a potential substrate of TRP14. We now show the molecular mechanism by which NF-κB activation is redox-dependently regulated through LC8. LC8 inhibited TNFα-induced NF-κB activation in HeLa cells by interacting with IκBα and thereby preventing its phosphorylation by IκB kinase (IKK), without affecting the activity of IKK itself. TNFα induced the production of reactive oxygen species, which oxidized LC8 to a homodimer linked by the reversible formation of a disulfide bond between the Cys[2] residues of each subunit and thereby resulted in its dissociation from IκBα. Butylated hydroxyanisol, an antioxidant, and diphenyleneiodonium, an inhibitor of NADPH oxidase, attenuated the phosphorylation and degradation of IκBα by TNFα stimulation. In addition LC8 inhibited NF-κB activation by other stimuli including interleukin-1β and lipopolysaccharide, both of which generated reactive oxygen species. Furthermore, TRP14 catalyzed reduction of oxidized LC8. Together, our results indicate that LC8 binds IκBα in a redox-dependent manner and thereby prevents its phosphorylation by IKK. TRP14 contributes to this inhibitory activity by maintaining LC8 in a reduced state.

Dyneins are large multi-component complexes that function as microtubule-based molecular motors both in the cytoplasm and in flagella (1). Cytoplasmic dyneins participate in a variety of intracellular motile processes including mitosis and vesicular transport, whereas axonemal dyneins provide motive force for the beating of cilia and flagella. The 8-kDa dynein light chain (LC8, also known as DLC8 or DLC1) was originally identified in flagellar dynein of *Chlamydomonas* (2) and was subsequently found to be a component of cytoplasmic dynein motor (3). LC8 is widely expressed and highly conserved among species, with the *Chlamydomonas* and human proteins sharing 93% sequence identity (2–4). It also serves essential cellular functions. For instance, in *Drosophila*, a partial loss-of-function mutation in LC8 results in pleiotropic morphogenetic defects in bristle and wing development, female sterility, and disruption of sensory axon projections (5, 6). Furthermore, a null mutation results in massive cell death via the apoptotic pathway and consequent embryonic death. In addition to being an essential component of the dynein motor complex, LC8 binds to a large number of proteins with diverse biological functions (7). For example, LC8 associates with and inhibits the activity of neuronal nitric-oxide synthase, giving rise to its alternative designation as PIN (protein inhibitor of neuronal nitric-oxide synthase) (8). It also binds to IκBα (9), an inhibitor of NF-κB[4]; to Bim (Bcl-2-interacting mediator of cell death) and Bmf (Bcl-2-modifying factor) (10, 11), both of which are proapoptotic members of the Bcl-2 family of proteins; to p21-activated kinase 1 (12, 13); and to p53-binding protein 1 (14).

The transcription factor NF-κB is a key regulator of immune and inflammatory responses and exists as a homo- or heterodimer composed of members of the Rel/NF-κB family of proteins, including RelA (p65), RelB, c-Rel, NF-κB1 (p105/p50), and NF-κB2 (p100/p52) (15). The most common form of NF-κB in mammalian cells is the heterodimer composed of RelA (p65) and p50 (16). Under basal conditions, NF-κB is present in the cytoplasm as an inactive complex with the inhibitor protein IκB. However, in response to a variety of stimuli, including TNFα, interleukin (IL)-1β, and lipopolysaccharide (LPS), IκBα is phosphorylated at residues Ser[32] and Ser[36] by IKK and then ubiquitinated at residues Lys[21] and Lys[22], result-

[1] Both authors contributed equally to this work.

[2] To whom correspondence may be addressed: Division of Life and Pharmaceutical Sciences, Ewha Womans University, Science Bldg. C, Rm. 102, 11-1 Daehyun-dong, Seodaemun-gu, Seoul 120-750, Korea. E-mail: rheesg@ewha.ac.kr.

[3] To whom correspondence may be addressed: Dept. of Life Science, Division of Life and Pharmaceutical Sciences, Ewha Woman's University, Science Bldg. C, Rm. 207, 11-1 Daehyun-dong, Seodaemun-gu, Seoul 120-750, Korea. Tel.: 82-2-3277-4495; Fax: 82-2-3277-3760; E-mail: jeongw@ewha.ac.kr.

[4] The abbreviations used are: NF-κB, nuclear factor κB; TNFα, tumor necrosis factor α; IKK, IκB kinase; ROS, reactive oxygen species; BHA, Butylated hydroxyanisol; DPI, diphenyleneiodonium; IL, interleukin; LPS, lipopolysaccharide; DTT, dithiothreitol; CM-H$_2$DCFDA, 5-(and-6)chloromethyl-2′,7′-dichlorodihydrofluorescein diacetate; MnSOD, Mn^{2+}-dependent superoxide dismutase; AEBSF, 4-(2-aminoethyl)benzene-sulfonyl fluoride; siRNA, small interfering RNA; AMS, 4-acetamido-4′-maleimidylstilbene-2,2′-disulfonate; Nox, NADPH oxidase; TrxR1, thioredoxin reductase 1; p-, phosphorylated; HA, hemagglutinin.

ing in its degradation by the 26 S proteasome (15). The degradation of IκBα exposes the nuclear localization signal of NF-κB, resulting in its translocation to the nucleus, where it regulates the transcription of various target genes that control the immune system, cell growth, and inflammation (17).

Recent findings suggest that ROS such as H_2O_2 activate NF-κB (18). The observations that potent NF-κB activators such as TNFα, IL-1β, and LPS trigger the production of ROS (19–22) and that a broad range of antioxidants inhibit NF-κB activation (23–25) suggest that most NF-κB inducers generate ROS, which mediate NF-κB activation cascade. The molecular mechanisms underlying these observations remain poorly understood, however, and the contribution of redox regulation to NF-κB activation remains unclear because of some conflicting reports (26, 27).

We recently showed that a novel disulfide reductase, TRP14, inhibits TNFα-induced NF-κB activation by suppressing the phosphorylation of IκBα, and we identified LC8 as a potential substrate of TRP14 (28). The proteins β-arrestin and κB-Ras inhibit NF-κB by interacting with IκBα and IκBβ, respectively (29–31), indicating that IκB-binding proteins are potentially important regulators of NF-κB function. We have therefore investigated whether LC8 might serve as a molecular intermediary that links the disulfide reductase activity of TRP14 to NF-κB regulation. We now show that LC8 inhibits IκBα phosphorylation by IKK through its redox-dependent interaction with IκBα and that TRP14 regulates this inhibitory activity by maintaining LC8 in a reduced state.

EXPERIMENTAL PROCEDURES

Reagents and Antibodies—LPS, butylated hydroxyanisol (BHA), diphenyleneiodonium (DPI), NADPH, and dithiothreitol (DTT) were obtained from Sigma; 4′,6-diamidino-2-phenylindole and 5-(and-6-)chloromethyl-2′,7′-dichlorodihydrofluorescein diacetate (CM-H_2DCFDA), acetyl ester were from Molecular Probes; MG132 was from Calbiochem; glutathione-Sepharose and nickel-chelating Sepharose were from Amersham Biosciences; and TNFα and IL-1β were from R & D Systems. Normal rabbit IgG was from Caltag Laboratories; mouse monoclonal and rabbit polyclonal antibodies to LC8 were from BD Biosciences and Phoenix Pharmaceuticals, respectively; rabbit antibodies to phosphorylated (p-) IκBα, to p-IKKα/β, and to IKKβ were from Cell Signaling Technology; a monoclonal antibody to p65 and rabbit polyclonal antibodies to IκBα and to IKKγ were from Santa Cruz Biotechnology; a monoclonal antibody to β-actin was from Abcam; rabbit polyclonal antibody to Mn^{2+}-dependent superoxide dismutase (MnSOD) was from Upstate Biotechnology; a monoclonal antibody to the FLAG epitope was from Sigma; and a rat antibody to the hemagglutinin (HA) epitope was from Roche Applied Science. Horseradish peroxidase-conjugated goat antibodies to rabbit or mouse IgG were from Amersham Biosciences Bioscience, and Alexa Fluor 488-conjugated monoclonal IgG was from Molecular Probes.

Cloning and Mutagenesis of Human LC8 cDNA—A mammalian expression vector for LC8, pFLAG-LC8, was described previously (28). Cysteine mutants of LC8 (C2S, C24S, and C56A, in which Cys^2, Cys^{24}, and Cys^{56} are individually replaced by serine

or alanine) were generated with the use of a site-directed mutagenesis kit (Stratagene) and complementary primers containing a 1-bp mismatch that converts the codon for cysteine to one for serine or alanine. To express HA-LC8 or LC8-FLAG proteins, cDNAs for wild-type LC8 or cysteine mutants of LC8 were cloned into the XbaI and BamHI sites of pCGN or into the EcoRI and BamHI sites of pFLAG-CMV5.1, respectively. For expression of LC8 in bacteria, the human LC8 gene was cloned into the NdeI and EcoRI sites of pET15b or pET17b.

Preparation of Recombinant Proteins—*Escherichia coli* BL21(DE3) transformed with pET17b-LC8 was cultured at 37 °C in LB medium supplemented with ampicillin (100 μg/ml). Isopropyl-β-ᴅ-thiogalactopyranoside was added to the culture at a final concentration of 0.4 mᴍ when the optical density at 600 nm had reached 0.5. After incubation for an additional 3 h, the cells were harvested by centrifugation and stored at −70 °C until use. The frozen cells were suspended in a solution containing 20 mᴍ Tris-HCl (pH 8.0), 1 mᴍ EDTA, and 1 mᴍ 4-(2-aminoethyl)benzene-sulfonyl fluoride (AEBSF) and were disrupted by sonication. After the removal of debris by centrifugation, the remaining soluble fraction was applied at a flow rate of 2 ml/min to a DEAE-Sepharose column that had been equilibrated with a solution containing 20 mᴍ Tris-HCl (pH 8.0) and 1 mᴍ EDTA. The flow-through fraction was collected and then applied to a gel filtration column (G3000SW; Tosoh Bioscience) that had been equilibrated with a solution containing 50 mᴍ HEPES-NaOH (pH 7.0) and 0.1 ᴍ NaCl. The fractions containing LC8 were pooled and dialyzed against 10 mᴍ HEPES-NaOH (pH 7.0). For the bacterial expression of IκBα, a DNA fragment encoding human IκBα was amplified by PCR from HeLa cell cDNA and cloned into the NdeI and BamHI sites of pET14b. His$_6$-tagged IκBα was purified from lysates of the transformed *E. coli* cells by affinity chromatography on nickel-chelating Sepharose.

In Vitro Kinase Assay—The phosphorylation of IκBα (1 μg) was performed for 30 min at 30 °C with an IKK immune complex in a final volume of 40 μl containing 50 mᴍ Tris-HCl (pH 7.5), 1 mᴍ EDTA, 5 mᴍ DTT, 1 mᴍ $MgCl_2$, 1 mᴍ Na_3VO_4, 5 mᴍ glycerophosphate, 100 μᴍ ATP, and 10 μCi of [γ-^{32}P]ATP. IκBα and LC8 were incubated for 30 min at 30 °C before the addition of the IKK complex. The IKK complex was isolated by immunoprecipitation with antibody to IKKγ and protein A-Sepharose from HeLa cells that had been exposed to TNFα (20 ng/ml) for 10 min. The kinase reaction mixtures were fractionated by SDS-PAGE on a 4–20% gradient gel, and the radioactivity associated with IκBα band was quantified with the use of a phosphorimaging device (Molecular Dynamics).

NF-κB Reporter Assay—NF-κB activity was measured with the use of a dual luciferase reporter assay system. The cells were transfected for 24 h with 0.25 μg of pNF-κB-Luc (NF-κB reporter plasmid; Stratagene), 0.25 μg of pRL-SV40 (internal control), and either pFLAG-CMV2 or pFLAG-LC8. The total amount of plasmid DNA was adjusted with pFLAG-CMV2. A dual luciferase assay was subsequently performed with a kit (Promega). The activity of firefly luciferase was normalized by that of the *Renilla* enzyme and was then expressed as fold increase relative to the normalized value for cells transfected with pFLAG-CMV2.

Depletion of LC8 by RNA Interference—A small interfering RNA (siRNA) corresponding to nucleotides 315–333 (relative to the translation initiation site) of human LC8 cDNA (5′-GGACT-GCAGCCTAAATTCC-3′) was synthesized with T7 RNA polymerase (32) and was introduced into HeLa cells with the use of Oligofectamine (Invitrogen) as described (28).

RNA Isolation, Reverse Transcription, and Real Time PCR Analysis—Cells that had been stimulated with TNFα (20 ng/ml) for 1 h were harvested, and total RNA was isolated1 with the use of the TRIzol reagent (Invitrogen) and quantified by measurement of absorbance at 260 nm. Reverse transcription was performed with 2 µg of total RNA and Moloney murine leukemia virus reverse transcriptase (Promega) for 1 h at 42 °C followed by 10 min at 70 °C, and the resulting cDNAs were subjected to real time PCR analysis with primers (sense and antisense, respectively) for human IκBα (5′-GCTGAAGAAG-GAGCGGCTACT-3′ and 5′-TCGTACTCCTCGTCTTTCAT-GGAC-3′), human IL-8 (5′-ATGACTTCCAAGCTGGCCGT-3′ and 5′-TTACATAATTTCTGTGTTGGC-3′), human cyclooxygenase-2 (5′-CCTTCCTCCTGTGCCTGATG-3′ and 5′-ACA-ATCTCATTTGAATCAGGAAGCT-3′), and human β-actin (5′-ATGAGCTGCGTGTGGCTC-3′ and 5′-GGCGTACAG-GGATAGCAC-3′). PCRs were performed with an ABI Prism 7300 sequence detection system and SYBRGreen PCR Master Mix (Applied Biosystems).

Determination of Redox Status of LC8—HeLa cells in six-well plates were washed with ice-cold phosphate-buffered saline and exposed directly to 10% trichloroacetic acid to prevent further oxidation. The precipitates were washed with 10% trichloroacetic acid and with acetone and were then suspended in 100 µl of reaction buffer (100 mM Tris-HCl, pH 8.8, 1 mM EDTA, 1.5% SDS, 1 mM AEBSF, leupeptin (10 µg/ml), aprotinin (10 µg/ml)) containing 20 mM 4-acetamino-4′-maleimidylstilbene-2,2′-disulfonate (AMS) or 40 mM N-ethylmaleimide. The reaction mixtures were incubated for 90 min at 30 °C, after which the reaction was stopped by the addition of 25 µl of 5× nonreducing SDS-PAGE sample buffer. AMS and N-ethylmaleimide were used to mask free thiol groups.

RESULTS

LC8 Interacts with IκBα and Thereby Inhibits Its Phosphorylation by IKK—Although LC8 was previously shown to interact physically with the regulatory domain of IκBα (9), the physiological function of this association has remained unknown. We first confirmed the interaction between LC8 and IκBα in HeLa cells by immunoprecipitation with antibody to IκBα. Not only transiently expressed FLAG-LC8 but also endogenous LC8 was immunoprecipitated together with IκBα (Fig. 1A). To examine whether LC8 inhibits IκBα phosphorylation by IKK, we assayed the kinase activity of the immunoprecipitated IKK complex with recombinant IκBα as the substrate in the presence of LC8. LC8 indeed inhibited the phosphorylation of IκBα by the IKK complex (Fig. 1B).

LC8 Expression Inhibits TNFα-induced NF-κB Activation—Given that LC8 inhibited IKK-mediated phosphorylation of IκBα *in vitro*, we next investigated the effect of forced expression of LC8 on the NF-κB signaling pathway in HeLa cells. Expression of FLAG-LC8 inhibited NF-κB activation by TNFα
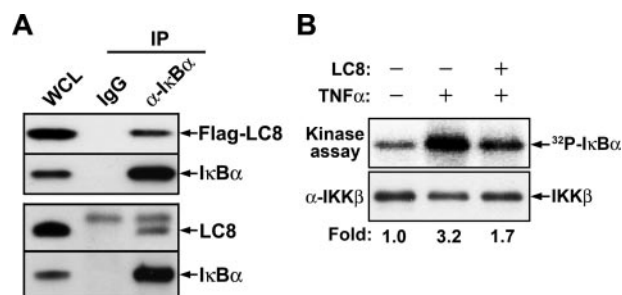

FIGURE 1. **Interaction of LC8 with IκBα and its inhibition of IκBα phosphorylation by IKK.** *A,* association of LC8 with IκBα. HeLa cells transfected for 24 h with pFLAG-LC8 were lysed in phosphate-buffered saline containing 1 mM EDTA, 0.5% Nonidet P-40, 1 mM AEBSF, aprotinin (10 µg/ml), and leupeptin (10 µg/ml). The cell lysates were incubated with normal rabbit IgG or antibody to IκBα (α-IκBα) for 2 h at 4 °C, and the immune complexes were then precipitated with protein A-Sepharose. Whole cell lysate (*WCL*) and immunoprecipitates (*IP*) were subjected to immunoblot analysis with antibodies to FLAG or to IκBα (*upper panel*). Alternatively, lysates of nontransfected HeLa cells were similarly subjected to immunoprecipitation, and endogenous LC8 was detected with antibody to LC8 (*lower panel*). *B,* inhibition by LC8 of IκBα phosphorylation mediated by IKK *in vitro*. An in vitro kinase assay was performed with recombinant IκBα, with IKK immunoprecipitated from cells treated (or not) with TNFα, and in the absence or presence of LC8, as described under "Experimental Procedures". The relative activities of IKK were determined from the radioactivity (^{32}P) associated with IκBα bands. The reaction mixtures were also subjected to immunoblot analysis with antibody to IKKβ.

in a concentration-dependent manner (Fig. 2A) as well as attenuated the TNFα-induced nuclear translocation of RelA (p65) (Fig. 2B). To determine which step of the NF-κB signaling pathway is influenced by LC8, we transfected cells with an expression vector for LC8 together with those for IKKβ or p65. LC8 inhibited the increase in NF-κB activity induced by IKKβ overexpression but not that attributable to overproduction of p65 (Fig. 2C), indicating that LC8 inhibits the NF-κB signaling pathway at a step between IKK activation and p65 nuclear translocation. However, the IKK complexes immunoprecipitated from cells transfected with the LC8 expression vector or the corresponding empty vector showed no difference in kinase activity measured *in vitro* with recombinant IκBα as the substrate (Fig. 2D). These results thus suggested that the binding of LC8 to IκBα inhibits its phosphorylation by IKK, without perturbing the activity of IKK itself, in TNFα-treated cells.

Depletion of LC8 Promotes TNFα-induced NF-κB Activation—To investigate the role of endogenous LC8 in TNFα-induced NF-κB activation, we depleted HeLa cells of LC8 by RNA interference and then monitored the expression of endogenous MnSOD, which is induced in response to NF-κB activation (33). The amount of LC8 was reduced by >90% after transfection of cells for 60 h with an siRNA specific for LC8 mRNA, compared with that apparent in cells transfected with a control RNA. Such depletion of LC8 resulted in a ~2-fold increase in the abundance of MnSOD in unstimulated cells and a 1.8-fold increase in TNFα-stimulated cells (Fig. 3A). We also determined the effect of LC8 depletion on the transcriptional induction of the NF-κB target genes for IκBα, cyclooxygenase-2, and IL-8 by reverse transcription and real time PCR analysis. Depletion of LC8 markedly increased the amounts of the target gene mRNAs under both basal and TNFα-stimulated conditions (Fig. 3B). In addition, depletion of LC8 promoted the nuclear translocation of p65 stimulated by TNFα (Fig. 3C). These data
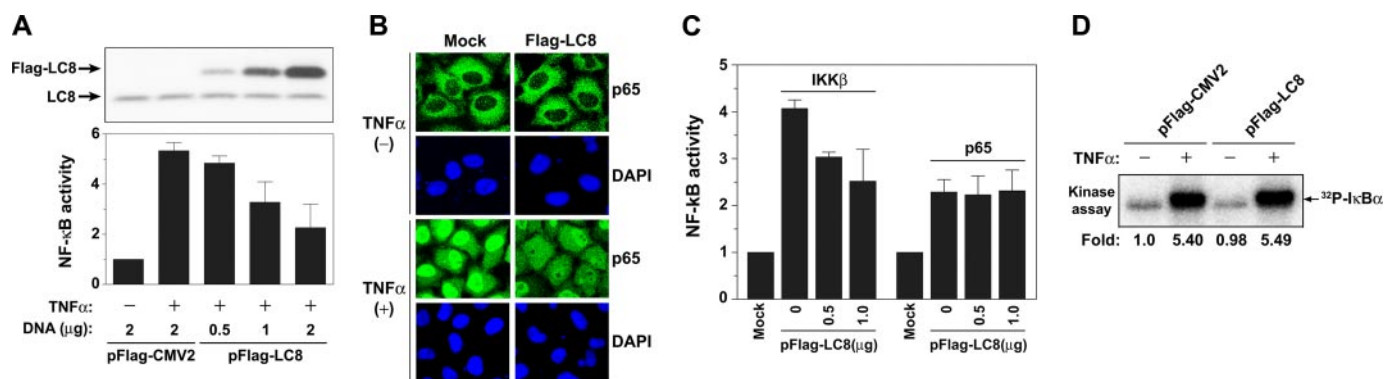
FIGURE 2. **Inhibition of TNFα-induced NF-κB activation by LC8 overexpression.** *A*, HeLa cells were transfected for 24 h with either pFLAG-CMV2 (2 μg) or the indicated amounts of pFLAG-LC8, with 0.25 μg of pNF-κB-Luc (NF-κB reporter plasmid), and with 0.25 μg of pRL-SV40 (internal control). The cells were incubated in the absence or presence of TNFα (20 ng/ml) for 6 h, after which the luciferase activities of cell lysates were measured with a dual luciferase assay system as described under "Experimental Procedures" (*lower panel*); the data are the means ± S.D. of values from three independent experiments. Cell lysates from a representative experiment were also subjected to immunoblot analysis with antibody to LC8 (*upper panel*). *B*, HeLa cells transfected with either pFLAG-CMV2 (Mock) or pFLAG-LC8 for 24 h were grown on coverslips, incubated in the absence or presence of TNFα (10 ng/ml) for 15 min, and fixed with 4% paraformaldehyde. They were then subjected to immunofluorescence staining with antibody to p65 as well as to staining of nuclei with 4',6-diamidino-2-phenylindole. *C*, HeLa cells were transfected with 1 μg of expression vectors for IKKβ or p65 as well as with pNF-κB-Luc, pRL-SV40, and the indicated amounts of pFLAG-LC8. They were harvested after 36 h for assay of luciferase activities. The data are the means ± S.D. of values from three independent experiments. *D*, HeLa cells were transfected with pFLAG-CMV2 or pFLAG-LC8 for 36 h and then incubated in the absence or presence of TNFα (20 ng/ml) for 10 min. The IKK complex was immunoprecipitated from cell lysates and assayed for kinase activity *in vitro* with IκBα as substrate as in Fig. 1*B*.
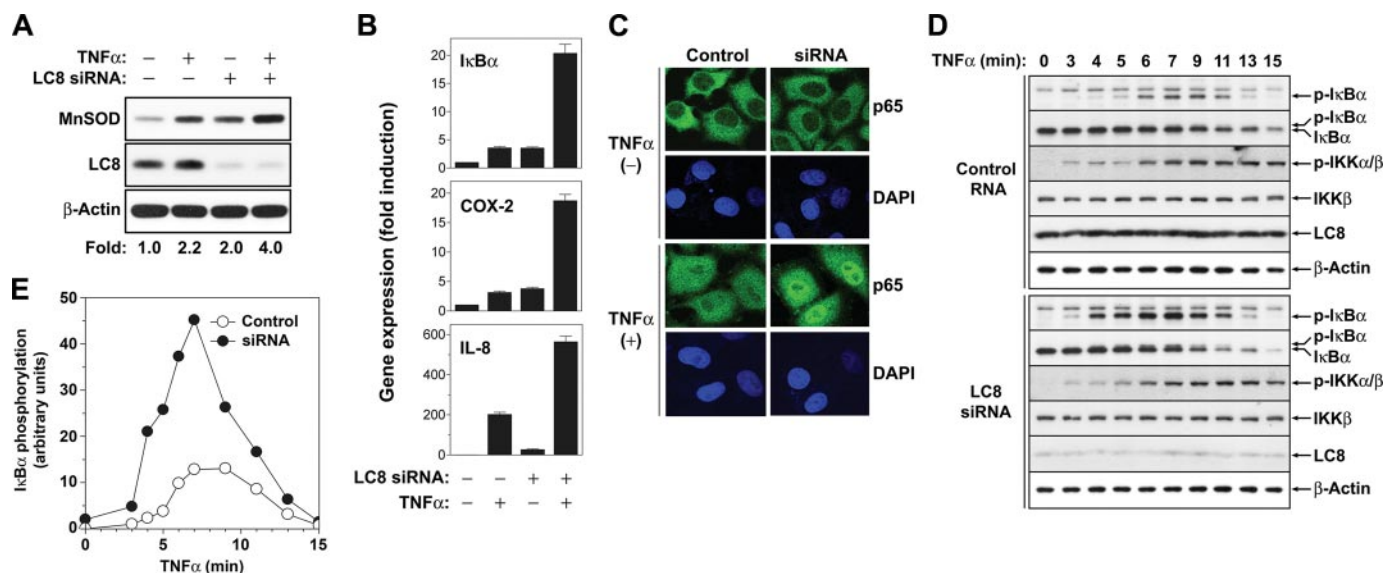
FIGURE 3. **Augmentation of TNFα-induced NF-κB activation by depletion of LC8.** *A*, HeLa cells were transfected for 60 h with LC8 siRNA or a control RNA and were then incubated in the absence or presence of TNFα (20 ng/ml) for 6 h. The abundance of MnSOD, LC8, and β-actin (loading control) in cell lysates was determined by immunoblot analysis. The intensity of the bands corresponding to MnSOD was normalized by that of the corresponding β-actin bands. *B*, HeLa cells were transfected as in *A* and incubated in the absence or presence of TNFα (20 ng/ml) for 1 h, after which total RNA was extracted from the cells and subjected to reverse transcription and real time PCR analysis to quantify the relative amounts of IκBα, cyclooxygenase-2, and IL-8 mRNAs. The data were normalized by the corresponding amount of β-actin mRNA and are the means ± S.D. of values from three independent experiments. *C*, HeLa cells were transfected as in *A*, incubated in the absence or presence of TNFα (10 ng/ml) for 7 min, fixed with 4% paraformaldehyde, and subjected to immunofluorescence staining as in Fig. 2*B*. *D* and *E*, HeLa cells transfected with LC8 siRNA as in *A* were incubated with TNFα (20 ng/ml) for the indicated times, after which cell lysates were subjected to immunoblot analysis with antibodies to p-IκBα, IκBα, p-IKKα/β, IKKβ, LC8, and β-actin (*D*). The chemiluminescence signals for p-IκBα were quantified and normalized by those of β-actin (*E*).

indicated that depletion of LC8 augments TNFα-induced NF-κB activation.

In response to activation signals such as TNFα, IκBα is phosphorylated by IKK and subsequently degraded by the ubiquitin-proteasome system. We therefore examined the effect of LC8 depletion on IκBα phosphorylation and degradation in HeLa cells stimulated with TNFα. Transfection of cells with LC8 siRNA substantially increased the extent of serine phosphorylation of IκBα compared with that apparent in cells transfected with a control RNA, and this effect was accompanied by an

increase in the rate of IκBα degradation (Fig. 3, *D* and *E*). In contrast, depletion of LC8 had little effect on the phosphorylation status of IKK. These results suggested that LC8 blocks IκBα phosphorylation by IKK but does not inhibit the activity of IKK itself, consistent with the results shown in Fig. 2*D*.

LC8 Inhibits NF-κB Activation by Other Stimuli That Activate IKK—Our results suggested that LC8 inhibits NF-κB activation by interacting with IκBα and thereby preventing its phosphorylation by IKK. Given that IL-1β and LPS also induce IκBα phosphorylation by IKK during activation of NF-κB (15,
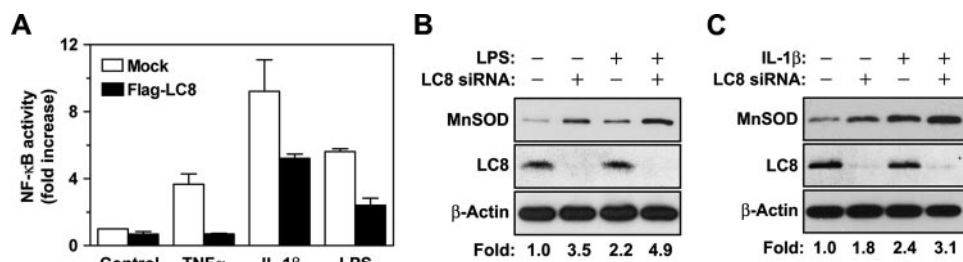
FIGURE 4. **Inhibition by LC8 of NF-κB activation induced by IL-1β or LPS.** *A*, HeLa, HEK293, and Raw 264.7 cells were transfected for 24 h with pNF-κB-Luc and pRL-SV40 as well as with pFLAG-CMV2 (Mock) or pFLAG-LC8. HeLa cells were then stimulated with TNFα (10 ng/ml) for 12 h, HEK293 cells were incubated with IL-1β (4 ng/ml) for 8 h, and Raw 264.7 cells were exposed to LPS (100 ng/ml) for 12 h. The cells were then harvested for assay of luciferase activities. The data are the means ± S.D. of values from three independent experiments. *B* and *C*, HeLa (*B*) or HEK293 (*C*) cells were transfected with LC8 siRNA or a control RNA for 60 h and were then either incubated in the absence or presence of LPS (100 ng/ml) for 12 h (*B*) or of IL-1β (10 ng/ml) for 6 h (*C*). The cell lysates were then analyzed for MnSOD expression as in Fig. 3*A*.
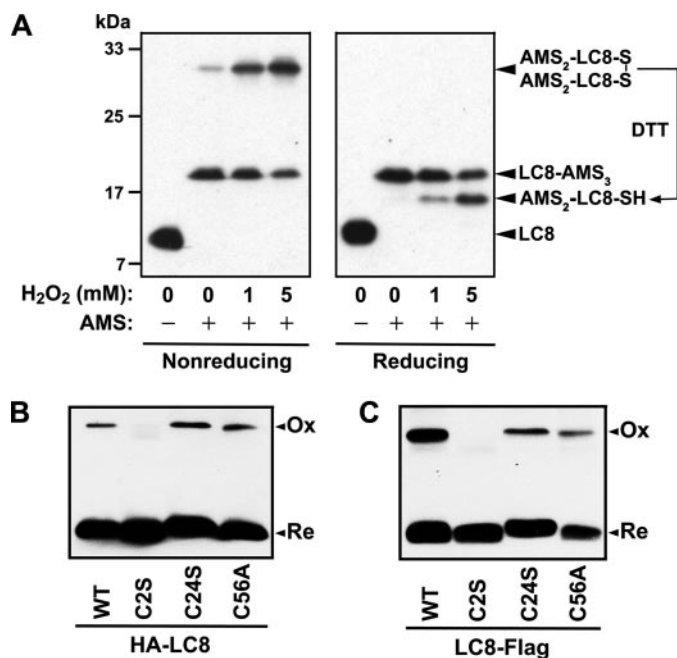
FIGURE 5. **Reversible formation of an intermolecular disulfide bond by LC8 on oxidation.** *A*, HeLa cells in six-well plates were transfected for 24 h with 1 μg of pFLAG-LC8 and then incubated with the indicated concentrations of H_2O_2 for 5 min. Free sulfhydryl groups of cellular proteins were masked with AMS as described under "Experimental Procedures," and the samples were then subjected to SDS-PAGE under nonreducing (*left panel*) or reducing (*right panel*) conditions followed by immunoblot analysis with antibody to FLAG. *B* and *C*, HeLa cells were transfected for 24 h with expression vectors for wild-type (*WT*) or cysteine mutant forms of LC8 tagged with HA at the NH₂ terminus and were then incubated in the presence of 1 mM H_2O_2 for 5 min (*B*). Alternatively, COS7 cells were transfected for 48 h with expression vectors for the cysteine mutants of LC8 tagged with FLAG at the COOH terminus and were then exposed to 1 mM H_2O_2 for 10 min (*C*). The samples were prepared and analyzed under nonreducing conditions as in *A*, with the exception that *N*-ethylmaleimide was used instead of AMS and that antibody to HA was used to detect HA-LC8. *Ox* and *Re* indicate the oxidized and reduced forms of LC8, respectively.

34), we examined whether LC8 inhibits NF-κB activation by these stimuli. The NF-κB reporter assay showed that forced expression of LC8 inhibited NK-κB activation induced by IL-1β or LPS (Fig. 4*A*). We also examined the effects of endogenous LC8 on NF-κB activation by LPS or IL-1β. Depletion of LC8 by RNA interference increased MnSOD expression in unstimulated or LPS-stimulated HeLa cells (Fig. 4*B*), as well as in

unstimulated or IL-1β-stimulated HEK293 cells (Fig. 4*C*). These results thus suggested that LC8 blocks IκBα phosphorylation by IKK in the canonical NF-κB activation pathway.

LC8 Forms a Reversible Intermolecular Disulfide Bond between Cys²\ Residues on Oxidation—LC8 was identified as a potential substrate for the novel disulfide reductase TRP14 in a substrate-trapping experiment on the basis of its formation of a mixed disulfide linkage with TRP14 (28), suggesting that LC8 likely forms a disulfide bond on oxidation. LC8 exists as a dimer under physiological conditions (35), and the human protein contains three cysteine residues (Cys^2, Cys^{24}, and Cys^{56}). To determine whether LC8 forms a disulfide bond on exposure of cells to H_2O_2, we analyzed its redox status by nonreducing SDS-PAGE after modification of free thiol groups with AMS. Alkylation of thiol groups with AMS increases the molecular mass of the host protein by 490 Da/thiol, resulting in a mobility shift on SDS-PAGE that allows determination of the number of oxidized cysteine residues (36). AMS modification of LC8 in unstimulated HeLa cells gave rise to two LC8 bands with markedly retarded electrophoretic mobility in nonreducing SDS-PAGE gels (Fig. 5*A*); the lower of these two bands appeared to correspond to a fully reduced form of LC8 ($LC8-AMS_3$), whereas the upper band seemed to represent an intermolecular disulfide-linked form (AMS_2-LC8-S-S-LC8-AMS_2). The intensity of the upper band was increased by exposure of the cells to H_2O_2 in a concentration-dependent manner. Under reducing conditions, the upper band was shifted to a position below the lower band ($LC8-AMS_3$) that appeared to correspond to AMS_2-LC8-SH (Fig. 5*A*). These results indicated that oxidation of LC8 results in the reversible formation of an intermolecular disulfide bond.

We next investigated which of the three cysteine residues (Cys^2, Cys^{24}, or Cys^{56}) of LC8 contribute to formation of the intermolecular disulfide bond. We substituted each cysteine residue with either serine or alanine by site-directed mutagenesis and then analyzed the oxidation status of the cysteine mutants in cells exposed to H_2O_2. Given that LC8 forms an intermolecular disulfide bond, we monitored the levels of disulfide-linked dimer by nonreducing SDS-PAGE after masking of free sulfhydryl groups with *N*-ethylmaleimide to prevent random disulfide bond formation. The C24S and C56A mutants formed the intermolecular disulfide bond, as did wild-type LC8, whereas the C2S mutant did not (Fig. 5*B*), suggesting that two Cys^2 residues form the disulfide linkage on oxidation of LC8 to the homodimer. It was possible that the environment surrounding the Cys^2 residue of recombinant LC8 was affected by the NH₂-terminal HA tag, which may have led to artifactual results. To exclude this possibility, we examined the oxidation status of COOH-terminally tagged LC8 (LC8-FLAG). Substitution of Cys^2 with serine also abolished intermolecular disulfide bond formation by LC8-FLAG (Fig. 5*C*).

Interaction between LC8 and IκBα Is Redox-dependent—In addition to LC8 being identified as a potential substrate of TRP14, this disulfide reductase was shown to inhibit the TNFα-induced activation of NF-κB (28). Our results showing that LC8 inhibits NF-κB by interacting with IκBα and thereby preventing its phosphorylation by IKK thus implicated LC8 as a molecular intermediary that links the reductase activity of TRP14 to NF-κB regulation. Given that TNFα also increases the intracellular generation of ROS (20), we examined whether TNFα induces LC8 oxidation. Stimulation of HeLa cells with TNFα resulted in a 2.2-fold increase in the intracellular level of ROS (Fig. 6A) as well as increased the amount of oxidized LC8 (Fig. 6B). This latter finding is consistent with the previous observation that LC8 formed a mixed disulfide intermediate with the C46S mutant of TRP14 in cells treated with TNFα (28). ROS generated in response to TNFα stimulation thus oxidized LC8 to an intermolecular disulfide-linked dimer that might then be reduced by TRP14.

To determine whether the association of LC8 with IκBα is redox-dependent, we examined the interactions of oxidized or reduced LC8 with His_6-IκBα with the use of a pulldown assay using nickel-chelating agarose. The proportion of LC8 precipitated with His_6-IκBα was markedly greater for the reduced form than for the oxidized form (Fig. 6C), suggesting that LC8 indeed interacts with IκBα in a redox-dependent manner. To examine whether the redox-dependent association of LC8 with IκBα also occurs in cells, we treated HeLa cells with H_2O_2 or TNFα in the presence of the proteasome inhibitor MG132 and then subjected cell lysates to immunoprecipitation with antibody to IκBα. Interaction between LC8 and IκBα was decreased greatly by exposure of cells to H_2O_2 and only slightly less so by treatment with TNFα, despite precipitation of similar amounts of IκBα from control and stimulated cells (Fig. 6D). These results suggested that ROS generated in response to TNFα stimulation oxidize LC8 and thereby induce its dissociation from IκBα.

Given that LC8 also inhibited NF-κB activation by LPS and IL-1β, both of which have been shown to trigger ROS generation (21, 22, 37), we also examined whether these NF-κB activators induced ROS production in the cells studied here. Indeed, LPS and IL-1β induced 10.2- and 3.5-fold increases, respectively, in the intracellular ROS level compared with that in control cells (Fig. 6, E and F). These results thus suggested that the inhibition by LC8 of NF-κB activation induced by LPS or IL-1β might also be regulated in a redox-dependent manner.

IκBα Phosphorylation Is Regulated in a Redox-dependent Manner—Our previous (28) and present results implicated TRP14 as an inhibitor of IκBα phosphorylation and showed that LC8 inhibits IKK-mediated IκBα phosphorylation through redox-dependent interaction with IκBα, respectively, in the pathway of TNFα-induced NF-κB activation. Together with the identification of LC8 as a potential substrate of TRP14 (28), these results suggested that IκBα phosphorylation may be regulated in a redox-dependent manner during TNFα-induced NF-κB activation. We therefore investigated the effect of the antioxidant BHA on TNFα-induced IκBα phosphorylation. The extent of TNFα-induced serine phosphorylation of IκBα was decreased in cells pretreated with BHA compared with that in cells not exposed to the antioxidant
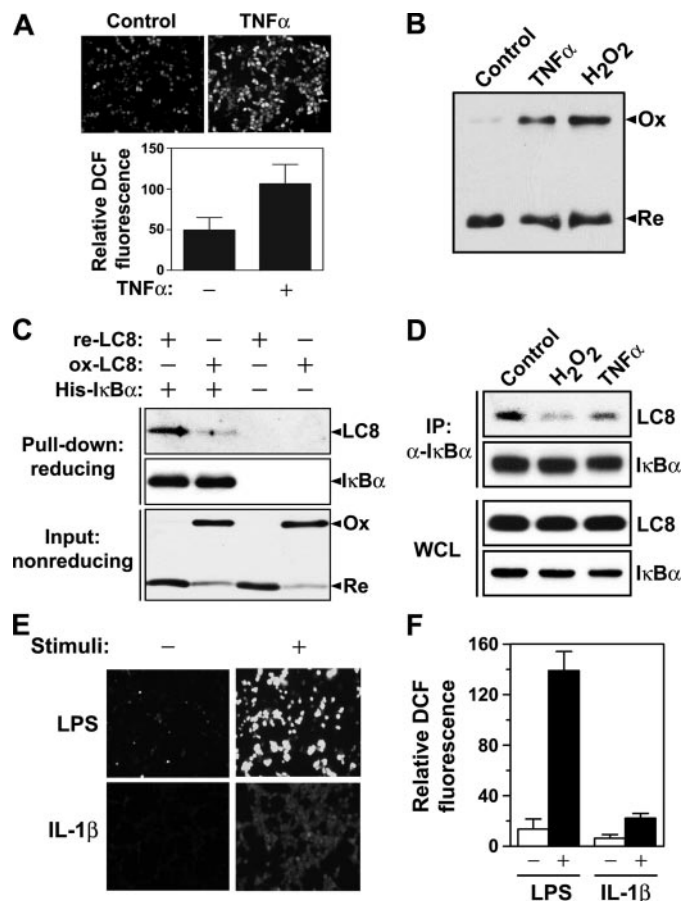
FIGURE 6. **Redox-dependent interaction of LC8 with IκBα.** *A*, HeLa cells were deprived of serum for 6 h in Dulbecco's modified Eagle's medium lacking phenol red, loaded with 2.5 μM CM-H_2DCFDA for 17 min, and then incubated in the absence or presence of TNFα (10 ng/ml) for 3 min. 2′,7′-dichlorofluorescein (DCF) fluorescence was visualized with a confocal laser-scanning microscope (*upper panels*). Relative fluorescence intensity per cell was measured by averaging the values for five groups of cells in each image and is presented as the means ± S.D. (*lower panel*). *B*, HeLa cells were transfected with pFLAG-LC8 for 24 h and then treated with TNFα (100 ng/ml) or 1 mM H_2O_2 for 10 min. The redox status of LC8 was analyzed as in Fig. 5B. *C*, recombinant LC8 (50 μM) was incubated with 1 mM DTT or 1 mM H_2O_2 for 1 h in a solution containing 20 mM Tris-HCl (pH 8.0) and 1 mM EDTA, after which the remaining DTT or H_2O_2 was immediately removed by ultrafiltration. His_6-tagged IκBα (1 μg) was incubated overnight at 4 °C with 1 μg of DTT-treated LC8 (*re-LC8*) or H_2O_2-treated LC8 (*ox-LC8*) in 0.5 ml of phosphate-buffered saline containing 0.5% Nonidet P-40, 1 mM AEBSF, aprotinin (10 μg/ml), and leupeptin (10 μg/ml). Protein complexes were then collected by incubation of the reaction mixtures with nickel-chelating Sepharose for 30 min at 4 °C followed by centrifugation, and they were subjected to immunoblot analysis with antibodies to LC8 and to IκBα (*upper panels*). The redox status of LC8 (*lower panel*) was also analyzed as in *B*. *D*, HeLa cells were exposed to 50 μM MG132 for 1 h and were then incubated in the absence or presence of 1 mM H_2O_2 or TNFα (100 ng/ml) for 10 min. Whole cell lysates (*WCL*) or immunoprecipitates (*IP*) prepared with antibody to IκBα as in Fig. 1A were subjected to immunoblot analysis of LC8 and IκBα. *E* and *F*, HEK293 cells were incubated overnight in Dulbecco's modified Eagle's medium supplemented with 0.5% fetal bovine serum. HEK293 or Raw 264.7 cells were incubated in Dulbecco's modified Eagle's medium without phenol red in the absence or presence of IL-1β (10 ng/ml) or LPS (1 μg/ml) for 30 min, respectively. After stimulation, the cells were immediately incubated with 2.5 μM CM-H_2DCFDA for 5 min, and 2′,7′-dichlorofluorescein fluorescence was then visualized with a confocal laser-scanning microscope (*E*). The relative fluorescence intensity per cell (*F*) was measured as in *A*.

(Fig. 7, *A* and *B*), and this effect was accompanied by a decrease in the rate of IκBα degradation (Fig. 7, *A* and *C*).

TNFα is known to produce ROS by activating NADPH oxidases (Noxs) in neutrophils, endothelial cells, and fibroblasts
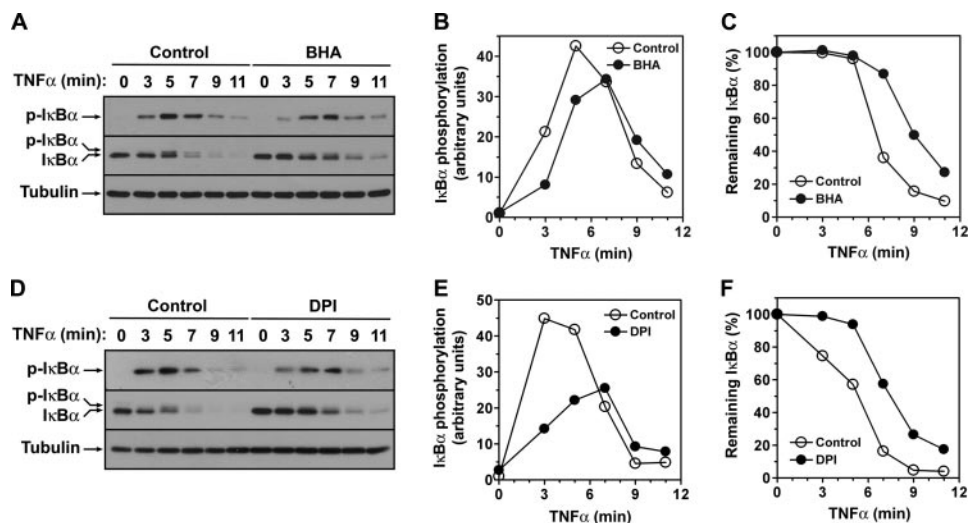
FIGURE 7. **Effects of BHA and DPI on the phosphorylation and degradation of IκBα during NF-κB activation by TNFα.** HeLa cells were incubated in the absence or presence of 100 μM BHA (*A–C*) or 10 μM DPI (*D–F*) for 30 min and were then stimulated with TNFα (20 ng/ml) in the continued absence or presence of the chemicals for the indicated times, after which cell lysates were prepared and subjected to immunoblot analysis with antibodies to p-IκBα, to IκBα, or to tubulin (loading control) (*A* and *D*). The chemiluminescence signals corresponding to p-IκBα (*B* and *E*) and to IκBα (*C* and *F*) were quantified, normalized by those of tubulin, and plotted.
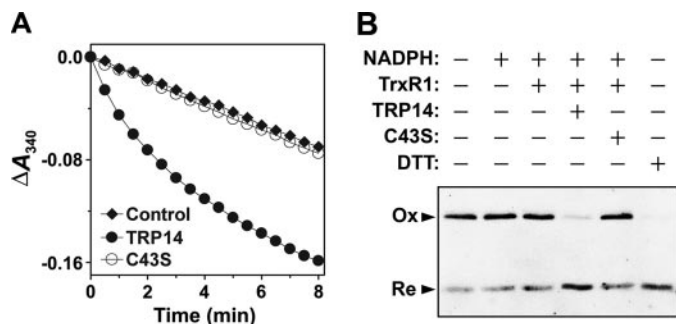
FIGURE 8. **Regulation of the redox status of LC8 by TRP14.** *A*, reduction of oxidized LC8 by TRP14 was assayed at 30 °C by monitoring A_{340} in a 0.2-ml reaction mixture containing 50 mM HEPES-NaOH (pH 7.0), 1 mM EDTA, 0.2 mM NADPH, 100 nM TrxR1, 170 μM oxidized LC8, and 10 μM TRP14 or TRP14-C43S. Oxidized LC8 was prepared as in Fig. 6*C*. A reaction mixture lacking TrxR1 served as a control. *B*, reduction of oxidized LC8 by TRP14 was initiated by the addition of oxidized LC8 at a final concentration of 50 μM to a reaction mixture containing 50 mM HEPES-NaOH (pH 7.0), 1 mM EDTA, 0.2 mM NADPH, 100 nM TrxR1, and 5 μM TRP14 or TRP14-C43S. The reaction was terminated after incubation for 30 min at 30 °C. As a positive control, 1 mM DTT was used for the reduction of oxidized LC8 under the same conditions. The redox status of LC8 was analyzed as in Fig. 6*C*. *Ox* and *Re* indicate the oxidized and reduced forms of LC8, respectively.

(19, 38–40). DPI, an inhibitor of flavin-containing enzymes, is widely used to inhibit Nox activity in cells. We therefore examined the effect of DPI on the serine phosphorylation and degradation of IκBα induced by TNFα (Fig. 7, *D–F*). The results were similar to those obtained in cells treated with BHA, suggesting that Nox-derived ROS are involved in the TNFα-induced phosphorylation of IκBα.

TRP14 Regulates the Redox Status of LC8—We previously showed that LC8 forms a mixed disulfide intermediate with the C46S mutant of TRP14, but not with wild-type TRP14, in cells treated with H_2O_2 or TNFα (28), suggesting that, under conditions of oxidative stress, intracellular LC8 forms a disulfide that is reduced by TRP14. We examined whether oxidized LC8 is reduced by TRP14 in the presence of rat thioredoxin reductase

1 (TrxR1) and NADPH by monitoring NADPH oxidation at 340 nm. Oxidized LC8 was indeed reduced by TRP14 but not by the catalytically inactive mutant TRP14-C43S (Fig. 8*A*). To confirm the reduction of oxidized LC8 by TRP14, we analyzed the redox status of LC8 by nonreducing SDS-PAGE after incubation of oxidized LC8 with TRP14. TRP14, but not TRP14-C43S, converted the oxidized LC8 dimer to the reduced monomer (Fig. 8*B*). These results thus suggest that TRP14 maintains LC8 in a reduced form and thereby contributes to the inhibition of NF-κB.

DISCUSSION

Although inhibitory effects of antioxidant proteins on NF-κB activation have been described (28, 41), little is known of the underlying molecular mechanisms. We have now revealed the molecular mechanism for redox-dependent regulation of NF-κB activation through LC8. We first showed that LC8 is a novel inhibitor of NF-κB. LC8 was thus found to prevent IκBα phosphorylation by IKK through interaction with IκBα, resulting in inhibition of NF-κB activation induced by TNFα. LC8 also inhibited NF-κB activation by other stimuli, including IL-1β and LPS that induce IκBα phosphorylation by IKK. LC8 thus likely serves as a common inhibitor in the canonical pathway of NF-κB activation mediated by IKK-dependent serine phosphorylation of IκBα.

We previously identified LC8 as a potential substrate of a novel disulfide reductase, TRP14, that regulates TNFα-induced NF-κB activation (28). We have now shown that LC8 interacts with IκBα in a redox-dependent manner and that TRP14 regulates the redox status of LC8. In cells exposed to TNFα or H_2O_2, LC8 was shown to form a reversible intermolecular disulfide linkage between the Cys^2 residues of each subunit of the homodimer and to dissociate from IκBα. All NF-κB activators examined in the present study (TNFα, IL-1β, and LPS) generated ROS, and TNFα-induced IκBα phosphorylation was inhibited by both the antioxidant BHA and the Nox inhibitor DPI. TRP14 also catalyzed the reduction of oxidized LC8. These observations suggest that IκBα phosphorylation is regulated in a redox-dependent manner by LC8, whose interaction with IκBα depends on its redox status, which in turn is modulated by cellular antioxidants such as TRP14.

Recently it has been reported that the ligated TNFα receptor forms a signaling complex harboring TRADD (TNF receptor-associated death domain protein), RIP1 (receptor interacting protein 1), NOXO1, the small GTPase Rac1, and Nox1, leading to the production of ROS in TNFα-stimulated mouse fibroblasts (19). TNFα is also known to be a potent activator of Nox2 in neutrophils and endothelial cells (38–40). On the basis of these observations together with our findings, we propose a tentative model for the redox regulation of NF-κB activation
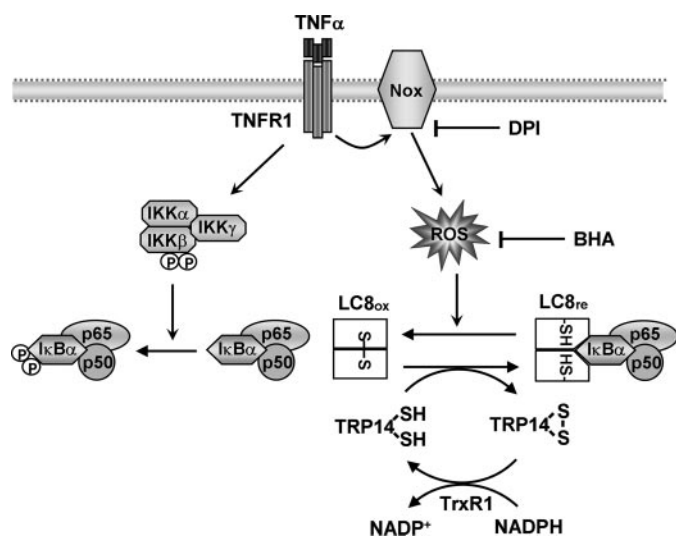
FIGURE 9. Model for the redox regulation of TNFα-induced NF-κB activation through LC8. See text for details.

through LC8 (Fig. 9). In resting cells, LC8 binds IκBα and inhibits IκBα phosphorylation by the IKK complex. Exposure of cells to TNFα triggers activation of the IKK complex and the production of ROS by activating a Nox enzyme. The transient ROS oxidize LC8 to a homodimer linked by a reversible intermolecular disulfide bond between the Cys^2 residues of each subunit, resulting in a conformational change and the dissociation of LC8 from IκBα. The released IκBα is then phosphorylated by the IKK complex and degraded by the 26 S proteasome. TRP14 contributes to LC8-mediated inhibition of NF-κB by maintaining LC8 in the reduced form, with TrxR1 and NADPH as a cellular source of reducing power. Antioxidants such as BHA and the Nox inhibitor DPI appear to inhibit IκBα phosphorylation by scavenging ROS and prohibiting ROS production, respectively. Given that IL-1β and LPS also triggered ROS generation and activated NF-κB in a manner sensitive to LC8, activation of NF-κB by these stimuli might also conform to this model. It has been reported that IL-1β and LPS induce the activation of Nox2 and Nox4, respectively (42, 43).

Our data support the notion that LC8 is a novel inhibitor of NF-κB and a target of redox regulation during NF-κB activation. In addition to the typical pathway of NF-κB activation elicited by TNFα, IL-1β, or LPS, atypical activation pathways have been described for UV, hypoxia reoxygenation, or pervanadate. UV induces phosphorylation of IκBα at a cluster of COOH-terminal sites by casein kinase II and subsequent IκBα degradation (44). Activation of NF-κB by hypoxia-reoxygenation or pervanadate depends on phosphorylation of IκBα at Tyr^{42} (45, 46). In addition, ROS have been increasingly recognized as critical components in the cellular response to stress-induced injury such as that caused by ischemia reperfusion or UV irradiation. It will therefore be of interest to determine whether LC8 also plays an inhibitory, redox-dependent role in atypical pathways of NF-κB activation.

Various proteins are known to interact with their binding partners in a redox-dependent manner. For example, reduced Trx1 associates with apoptosis signal-regulating kinase 1 and thereby inhibits its activity, but oxidized Trx1 does not (47, 48).

Such redox-dependent interaction is likely due to a conformational change according to redox status. Given that the two Cys^2 residues are positioned distant from each other in the crystal structure of the LC8 dimer (49), formation of an intermolecular disulfide bond between these two residues likely induces a large conformational change that results in disruption of the LC8-IκBα complex. Structural comparisons of reduced and oxidized LC8 proteins will likely provide insight into the redox-dependent interaction between LC8 and IκBα.

LC8 proteins of mammals, including human, cow, rat, mouse, and rabbit, contain three cysteine residues (Cys^2, Cys^{24}, and Cys^{56}). Both Cys^{24} and Cys^{56} are conserved from fruit fly to human, but Cys^2 is present only in mammalian LC8 proteins, suggesting that the redox-dependent association of LC8 with IκBα is likely limited to mammals. Two members of the LC8 family, LC8a (also known as LC8 or DLC1) and LC8b (also known as DLC2), are present in several mammalian species, and a third member, LC8c, is listed in the human sequence data base (4). Two proapoptotic members of the Bcl-2 family of proteins, Bim and Bmf, interact with LC8 family members (50). Whereas Bim is normally sequestered by the microtubule-associated dynein motor complex through its interaction with LC8a, Bmf is sequestered by the actin-based myosin V motor through association with LC8b. LC8b shares 93% sequence identity with LC8a but contains Ser^2 instead of Cys^2. It will therefore be of interest to examine whether LC8-mediated regulation of the proapoptotic activity of Bim is redox-dependent.

NF-κB plays a key role in osteoclast differentiation and chronic inflammatory diseases such as rheumatoid arthritis, asthma, inflammatory bowel disease, and psoriasis (51–53). It has also been implicated in other diseases including atherosclerosis, Alzheimer disease, and cancer (54–56). Given that total loss of LC8 function in *Drosophila* results in embryonic death (5), knock-out of LC8 in mice is also likely to be lethal. Further insight into the physiological functions of LC8 as a novel NF-κB inhibitor and into its potentially protective role in diseases such as osteoporosis, rheumatoid arthritis, and atherosclerosis will therefore likely be obtained by studies of LC8 transgenic mice.

REFERENCES
1. King, S. M. (2000) *Biochim. Biophys. Acta* **1496,** 60–75
2. King, S. M., and Patel-King, R. S. (1995) *J. Biol. Chem.* **270,** 11445–11452
3. King, S. M., Barbarese, E., Dillman, J. F., III, Patel-King, R. S., Carson, J. H., and Pfister, K. K. (1996) *J. Biol. Chem.* **271,** 19358–19366
4. Wilson, M. J., Salata, M. W., Susalka, S. J., and Pfister, K. K. (2001) *Cell Motil. Cytoskeleton* **49,** 229–240
5. Dick, T., Ray, K., Salz, H. K., and Chia, W. (1996) *Mol. Cell Biol.* **16,** 1966–1977
6. Phillis, R., Statton, D., Caruccio, P., and Murphey, R. K. (1996) *Development* **122,** 2955–2963
7. Fan, J., Zhang, Q., Tochio, H., Li, M., and Zhang, M. (2001) *J. Mol. Biol.* **306,** 97–108
8. Jaffrey, S. R., and Snyder, S. H. (1996) *Science* **274,** 774–777
9. Crepieux, P., Kwon, H., Leclerc, N., Spencer, W., Richard, S., Lin, R., and Hiscott, J. (1997) *Mol. Cell Biol.* **17,** 7375–7385
10. Puthalakath, H., Huang, D. C., O'Reilly, L. A., King, S. M., and Strasser, A. (1999) *Mol. Cell* **3,** 287–296

11. Puthalakath, H., Villunger, A., O'Reilly, L. A., Beaumont, J. G., Coultas, L., Cheney, R. E., Huang, D. C., and Strasser, A. (2001) *Science* **293,** 1829 –1832

12. Vadlamudi, R. K., Bagheri-Yarmand, R., Yang, Z., Balasenthil, S., Nguyen, D., Sahin, A. A., den Hollander, P., and Kumar, R. (2004) *Cancer Cell* **5,** 575–585

13. Lu, J., Sun, Q., Chen, X., Wang, H., Hu, Y., and Gu, J. (2005) *Biochem. Biophys. Res. Commun.* **331,** 153–158

14. Lo, K. W., Kan, H. M., Chan, L. N., Xu, W. G., Wang, K. P., Wu, Z., Sheng, M., and Zhang, M. (2005) *J. Biol. Chem.* **280,** 8172–8179

15. Hayden, M. S., and Ghosh, S. (2004) *Genes Dev.* **18,** 2195–2224

16. Baldwin, A. S., Jr. (1996) *Annu. Rev. Immunol.* **14,** 649 – 683

17. Pahl, H. L. (1999) *Oncogene* **18,** 6853 – 6866

18. Gloire, G., Legrand-Poels, S., and Piette, J. (2006) *Biochem. Pharmacol.* **72,** 1493–1505

19. Kim, Y. S., Morgan, M. J., Choksi, S., and Liu, Z. G. (2007) *Mol. Cell* **26,** 675– 687

20. Vlahopoulos, S., Boldogh, I., Casola, A., and Brasier, A. R. (1999) *Blood* **94,** 1878–1889

21. Li, Q., Harraz, M. M., Zhou, W., Zhang, L. N., Ding, W., Zhang, Y., Eggleston, T., Yeaman, C., Banfi, B., and Engelhardt, J. F. (2006) *Mol. Cell Biol.* **26,** 140 –154

22. Sanlioglu, S., Williams, C. M., Samavati, L., Butler, N. S., Wang, G., McCray, P. B., Jr., Ritchie, T. C., Hunninghake, G. W., Zandi, E., and Engelhardt, J. F. (2001) *J. Biol. Chem.* **276,** 30188 –30198

23. Garg, A. K., and Aggarwal, B. B. (2002) *Mol. Immunol.* **39,** 509 –517

24. Brigelius-Flohe, R., Banning, A., Kny, M., and Bol, G. F. (2004) *Arch. Biochem. Biophys.* **423,** 66 –73

25. Asehnoune, K., Strassheim, D., Mitra, S., Kim, J. Y., and Abraham, E. (2004) *J. Immunol.* **172,** 2522–2529

26. Bowie, A., and O'Neill, L. A. (2000) *Biochem. Pharmacol.* **59,** 13–23

27. Hayakawa, M., Miyashita, H., Sakamoto, I., Kitagawa, M., Tanaka, H., Yasuda, H., Karin, M., and Kikugawa, K. (2003) *EMBO J.* **22,** 3356 –3366

28. Jeong, W., Chang, T. S., Boja, E. S., Fales, H. M., and Rhee, S. G. (2004) *J. Biol. Chem.* **279,** 3151–3159

29. Witherow, D. S., Garrison, T. R., Miller, W. E., and Lefkowitz, R. J. (2004) *Proc. Natl. Acad. Sci. U. S. A.* **101,** 8603– 8607

30. Fenwick, C., Na, S. Y., Voll, R. E., Zhong, H., Im, S. Y., Lee, J. W., and Ghosh, S. (2000) *Science* **287,** 869 – 873

31. Huxford, T., and Ghosh, G. (2005) *Methods Enzymol.* **407,** 527–534

32. Donze, O., and Picard, D. (2002) *Nucleic Acids Res.* **30,** e46

33. Xu, Y., Kiningham, K. K., Devalaraja, M. N., Yeh, C. C., Majima, H., Kasarskis, E. J., and St Clair, D. K. (1999) *DNA Cell Biol.* **18,** 709 –722

34. Li, N., and Karin, M. (1998) *Proc. Natl. Acad. Sci. U. S. A.* **95,** 13012–13017

35. Benashski, S. E., Harrison, A., Patel-King, R. S., and King, S. M. (1997) *J. Biol. Chem.* **272,** 20929 –20935

36. Mezghrani, A., Fassio, A., Benham, A., Simmen, T., Braakman, I., and Sitia, R. (2001) *EMBO J.* **20,** 6288 – 6296

37. Tateishi, Y., Sasabe, E., Ueta, E., and Yamamoto, T. (2008) *Biochem. Biophys. Res. Commun.* **366,** 301–307

38. Frey, R. S., Rahman, A., Kefer, J. C., Minshall, R. D., and Malik, A. B. (2002) *Circ. Res.* **90,** 1012–1019

39. Dewas, C., Dang, P. M., Gougerot-Pocidalo, M. A., and El-Benna, J. (2003) *J. Immunol.* **171,** 4392– 4398

40. Dang, P. M., Stensballe, A., Boussetta, T., Raad, H., Dewas, C., Kroviarski, Y., Hayem, G., Jensen, O. N., Gougerot-Pocidalo, M. A., and El-Benna, J. (2006) *J. Clin. Investig.* **116,** 2033–2043

41. Hayashi, T., Ueno, Y., and Okamoto, T. (1993) *J. Biol. Chem.* **268,** 11380 –11388

42. Li, Q., and Engelhardt, J. F. (2006) *J. Biol. Chem.* **281,** 1495–1505

43. Park, H. S., Jung, H. Y., Park, E. Y., Kim, J., Lee, W. J., and Bae, Y. S. (2004) *J. Immunol.* **173,** 3589 –3593

44. Kato, T., Jr., Delhase, M., Hoffmann, A., and Karin, M. (2003) *Mol. Cell* **12,** 829 – 839

45. Imbert, V., Rupec, R. A., Livolsi, A., Pahl, H. L., Traenckner, E. B., Mueller-Dieckmann, C., Farahifar, D., Rossi, B., Auberger, P., Baeuerle, P. A., and Peyron, J. F. (1996) *Cell* **86,** 787–798

46. Fan, C., Li, Q., Ross, D., and Engelhardt, J. F. (2003) *J. Biol. Chem.* **278,** 2072–2080

47. Saitoh, M., Nishitoh, H., Fujii, M., Takeda, K., Tobiume, K., Sawada, Y., Kawabata, M., Miyazono, K., and Ichijo, H. (1998) *EMBO J.* **17,** 2596 –2606

48. Tobiume, K., Saitoh, M., and Ichijo, H. (2002) *J. Cell Physiol.* **191,** 95–104

49. Liang, J., Jaffrey, S. R., Guo, W., Snyder, S. H., and Clardy, J. (1999) *Nat. Struct. Biol.* **6,** 735–740

50. Puthalakath, H., and Strasser, A. (2002) *Cell Death Differ.* **9,** 505–512

51. Barnes, P. J., and Karin, M. (1997) *N. Engl. J. Med.* **336,** 1066 –1071

52. Jimi, E., Aoki, K., Saito, H., D'Acquisto, F., May, M. J., Nakamura, I., Sudo, T., Kojima, T., Okamoto, F., Fukushima, H., Okabe, K., Ohya, K., and Ghosh, S. (2004) *Nat. Med.* **10,** 617 – 624

53. McIntyre, K. W., Shuster, D. J., Gillooly, K. M., Dambach, D. M., Pattoli, M. A., Lu, P., Zhou, X. D., Qiu, Y., Zusi, F. C., and Burke, J. R. (2003) *Arthritis Rheum.* **48,** 2652–2659

54. Kutuk, O., and Basaga, H. (2003) *Trends Mol. Med.* **9,** 549 –557

55. Kaltschmidt, B., Uherek, M., Volk, B., Baeuerle, P. A., and Kaltschmidt, C. (1997) *Proc. Natl. Acad. Sci. U. S. A.* **94,** 2642–2647

56. Shishodia, S., and Aggarwal, B. B. (2004) *Biochem. Pharmacol.* **68,** 1071–1080